Mode-Matching Analysis of TE_{011}-Mode Waveguide Bandpass Filters

Andrea Melloni, Marco Politi, and Gian Guido Gentili

Abstract—**A mode-matching technique for the analysis of waveguide bandpass filters employing circular TE_{011} resonators, coupled by rectangular apertures, is presented. Such a technique takes rigorously into account thickness and angular offset of the two coupling irises, and higher modes interactions between resonators, while overcoming the typical limitations of the available approximate models. We show, through an optimization procedure, that it is possible to design filters with a desired frequency response, without needing any further empiric adjustments. Spurious responses can be controlled too.**

I. Introduction

THE HIGH unloaded Q-factor of TE_{011}-mode in cylindrical cavity is very attractive for the realization of low-loss narrow-band filters at millimeter wavelengths. Direct coupled filters employing this kind of resonators can be designed to have a very selective passband with steep skirts, together with a very low midband insertion loss. One further advantage is the higher midband pulse power capacity, when compared to other waveguide filters.

The main building block of the TE_{011}-mode bandpass filter is the cylindrical resonator shown in Fig. 1, coupled both with the external rectangular waveguides and with the adjacent cavities through two rectangular apertures (coupling irises) which are placed on the cavity sidewall with an angular offset equal to 2θ.

The analysis of such filters is usually performed with reference to approximate models based on "Bethe's small coupling theory" [1], later modified by Cohn [2], MacDonald [3], [4] and, recently, by Levy [5]. Such models cannot take into account the effects of the coupling apertures on the TE_{011} resonant frequency and the higher-order mode coupling between adjacent resonators and the irises angular offset 2θ. Moreover, the design of such filters [6,] [7] is complicated by the large number of spurious modes that resonate at frequencies that are close to the TE_{011} mode and its degeneracy with TM_{111} mode. As a result, several empirical adjustments may be required when bandpass filters are designed according to the approximate models, and particular care must be taken to guarantee satisfactory cavity tuning control and suppression of adjacent modes [8], [9].

This paper proposes a mode-matching technique for analyzing all buiding blocks of the above filter in order to accurately evaluate their frequency response. The resulting procedure allows the designer to take into account the effect of all coupling apertures, the angle 2θ between them (see Fig. 1), the spurious responses and the higher-order-mode interaction between adjacent resonators. The only restriction on the irises dimensions is that the aperture width b_i must be small compared to the diameter R of the cavity. Small values of the ratio b_i/R results in a considerable simplification of the mode-matching procedure. This, however, is not a severe restriction as the coupling mainly depends on a_i. If, for any reason, one has to use larger values of b_i, the more general mode-matching procedure reported in [10], [11] can be employed. The technique we propose is quite accurate up to $b_i/R \simeq 0.3$.

The method is explained in Section II-A for cavities coupled through irises with identical dimensions. The more general case of asymmetrical cavities having two different apertures is treated separately in Section II-B. An extensive convergence analysis has been carried out in Section III and the efficiency of the method and other numerical results are discussed in Section IV. Some prototype filters with one and four cavities have been built as well in order to validate the method described above. In these cases, a very good agreement between simulations and measurements has been observed, as discussed in Section V.

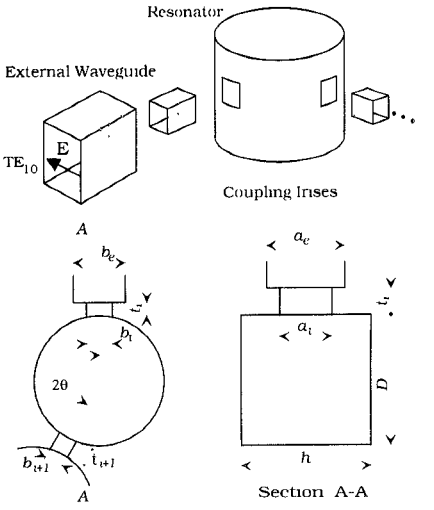

Fig. 1. The cylindrical resonator coupled to the external waveguides and to the adjacent resonators by rectangular coupling irises.

II. The Solution of the Field Problem

The analysis of the TE_{011} bandpass filter can be conveniently carried out by splitting the whole structure in simpler

Manuscript received November 10, 1994; revised May 25, 1995.

A. Melloni and M. Politi are with the Politecnico di Milano, Dipartimento di Elettronica e Informazione, I-20133 Milano, Italy.

G. G. Gentili is with the CSTS-CNR, Politecnico di Milano, Milano, Italy.

IEEE Log Number 9413430.

building blocks, as shown in Fig. 1. Only two discontinuities are present: the symmetrical double-step formed by the junction between the rectangular external waveguide and the first (last) rectangular coupling iris and the discontinuity at the junction between the irises and the cavity itself. Each discontinuity is considered separately and its generalized scattering matrix is evaluated. The overall scattering matrix of the total filter is then calculated by a suitable direct combination of all single scattering matrices [12].

In this work, the mode-matching technique is used to calculate the generalized scattering matrix of each discontinuity since it is a method particularly suitable when the fields in each region can be expressed analitically as a mode superposition. The first step of the mode-matching technique consists in choosing the most suitable modal expansion of the fields in the regions forming the junction. The analysis of double-step discontinuities in rectangular waveguide has been carried out by several authors. In the past [13], [14] the rigorous TE-TM field expansion was successfully used. Numerical analysis, however, has verified that the electric E_x component of the scattered field is much smaller than others in the bandwith of the dominant TE_{10} mode, suggesting a TE^x field expansion [15]–[17]. The TE^x expansion has the advantage of working with smaller matrices with respect to the TE-TM case, reducing the CPU time and storage requirements and it was therefore used in this work.

Let z be the direction of propagation in the rectangular region, that is the external waveguide and the coupling irises, as shown in Fig. 2. The modal expansions of the fields components are derived by an x-directed magnetic scalar potential $\Pi_x \hat{\mathbf{x}}$. The expressions of potential and fields, assuming a dependence of the type $e^{j\omega t}$, are the following

$$\Pi_x = \sum_q \frac{1}{\gamma_q}(a_q^+ e^{-\gamma_q z} - a_q^- e^{\gamma_q z})\phi_q^{\square}(x,y) \tag{1}$$

$$E_y^{\square} = -j\omega\mu\frac{\partial \Pi_x}{\partial z} = \sum_q (a_q^+ e^{-\gamma_q z} + a_q^- e^{\gamma_q z}) e_{yq} \tag{2}$$

$$H_x^{\square} = \left(k^2 + \frac{\partial^2}{\partial x^2}\right)\Pi_x = \sum_q (a_q^+ e^{-\gamma_q z} - a_q^- e^{\gamma_q z}) h_{xq} \tag{3}$$

where $\phi_q^{\square}$ is the rectangular mode function

$$\phi_q^{\square}(x,y) = \sqrt{\frac{2\epsilon_n}{ab}} \cos k_{xm} x \cos k_{yn}\left(\frac{b}{2} + y\right) \tag{4}$$

ϵ_n is the Neumann factor which equals 1 if $n = 0$ and 2 if $n \neq 0$ and a normalizing coefficient has been introduced so that $\int_S \phi_q^{\square 2}\, dS = 1$. q is some combination of m and n and $k = \omega\sqrt{\mu\varepsilon}$. The mark $^{\square}$ is used to distinguish quantities related to the rectangular region from quantities related to the circular one, indicated in the following with $^{\circ}$.

In (2), (3) the modal eigenfunctions are

$$e_{yq} = j\omega\mu\phi_q^{\square} \tag{5}$$

$$h_{xq} = (k^2 - k_{xm}^2)\phi_q^{\square}/\gamma_q \tag{6}$$

being $\gamma_q = \sqrt{k_{xm}^2 + k_{yn}^2 - k^2}$ the propagation constant, $k_{xm} = (2m+1)\pi/a$ and $k_{yn} = n\pi/b$ with $m, n = 0, 1, \ldots \infty$.

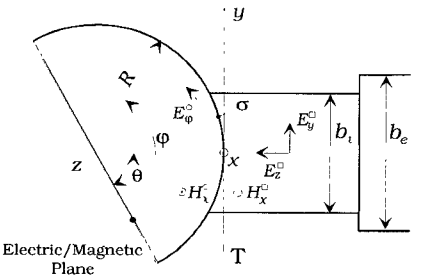

Fig. 2. Top view of the iris-cavity junction.

Finally a_q^+ and a_q^- are the incident and reflected modal coefficients, respectively.

Let's now concentrate on the fields modal expansion in the cylindrical cavity. The external waveguide operate in TE_{10} dominant mode and the coupling irises are below the cut off. Under these conditions, and due to the orientation of the waveguide itself (see Fig. 1), no E_x component exists in the coupling irises and hence only TE^x mode (simply TE in the following) are excited in the cavity.

In practice TM modes could be weakly excited because of unwanted asymmetries and losses, but in general their effects are negligible and they are not considered in the following. The TM_{111}-mode is the only one that can seriously affect the bandpass filter performance because it is degenerate with the TE_{011}-mode. This degeneracy can be split simply by using a noncontacting tuning plunger or by modifing the resonator as in [8, 9], but these are empirical adjustments and are not considered in this analysis.

The cavity can be considered as a radial waveguide of height h. The termination of such a waveguide with an ideal electric surface with two rectangular apertures at a distance R from the center of the cavity will be enforced later by the mode-matching technique. After that, the modal field components of interest in the cavity are [10], [18]

$$E_\varphi^\circ = j\omega\mu \sum_{p=1}^{\infty} c_p \phi_{p_m^e}^\circ(\varphi, x) \tag{7}$$

$$H_x^\circ = \sum_{p=1}^{\infty} c_p Y_p^\circ \phi_{p_m^e}^\circ(\varphi, x) \tag{8}$$

where

$$Y_p^\circ = \frac{\kappa_{cj} J_i(\kappa_{cj} R)}{J_i'(\kappa_{cj} R)} = \frac{\kappa_{cj}^2 R}{i - \kappa_{cj} R \frac{J_{i+1}(\kappa_{cj} R)}{J_i(\kappa_{cj} R)}} \tag{9}$$

being $\kappa_{cj} = \sqrt{k^2 - \kappa_{xj}^2}$, $\kappa_{xj} = j\pi/h$, and $i = 0, 1, \ldots \infty$, $j = 1, 2, \ldots \infty$ are integer numbers depending on p.

In (9) the ratio between the two first kind Bessel functions J of order $i+1$ and i can be easily calculated [19, p. 363]. Moreover c_p is the modal amplitude coefficient and $\phi_{p_m^e}^\circ(\varphi, x)$ is the modal eigenfunction

$$\phi_{p_m^e}^\circ(\varphi, x) = \sqrt{\frac{\epsilon_i}{hr\pi}} \cos(\kappa_{xj} x) \begin{matrix}\cos \\ \sin\end{matrix} (i\varphi) \tag{10}$$

where $\epsilon_i = 1$ if $i = 0$ and $\epsilon_i = 2$ otherwise. As for the eigenfunction of the rectangular waveguide, a normalizing

factor has been added so that $\int_S \phi^{\circ 2}_{p^e_m} dS = 1$ over the cavity sidewall S.

Note, by the way, that the field has been expanded in first kind Bessel functions. This physically means that the cavity fields are expanded in stationary modes and (7) and (8) represent the solution of the Helmholtz equation in cylindrical coordinates, once the singularity in $r = 0$ has been removed. Moreover modes with $\kappa_{xj} = 0$ do not satisfy the boundary condition on the bottom and the top of the cavity and they can be neglected.

Finally, if the coupling apertures are placed midheight on the cavity sidewall, only symmetrical modes with respect to the x direction have to be considered, that is $k_{xm} = (2m+1)\pi/a$, $\kappa_{xj} = (2j+1)\pi/h$ and $m, j = 0, 1, 2 \ldots \infty$.

In the next two sections the continuity of the fields in the apertures and the boundary condition on the metallic sidewall of the cavity permit the obtaining of the generalized scattering matrix of the resonator.

A. Symmetrical Cavity

A simple but important case is represented by a cavity with two identical apertures symmetrically placed with respect to the height of the cavity. Cavities with two different apertures are treated in the next section.

By taking advantage of symmetry, only half of a cavity, obtained by inserting either an electric or a magnetic wall at the symmetry plane, has to be analyzed. A top view of half of the cavity so obtained is shown in Fig. 2 together with the electric and magnetic field components to be matched. The two generalized one port scattering matrices of half the cavity are derivable by suitable projection of the E-field and H-field continuity equations over the aperture. If b_i is small compared with R, the derivation of the two equations is straightforward. This assumption means that the curvature of the matching surface, named σ in Fig. 2, can be neglected. The $E^{\square}_z$ electric field component in the iris is therefore neglected and the continuity between the cavity electric field E°_{φ} and the electric field component $E^{\square}_y$ in the rectangular aperture, tangential to σ, must be enforced, i.e.,

$$E^{\circ}_{\varphi} = \begin{cases} E^{\square}_y & \text{aperture} \\ 0 & \text{cavity sidewall} \end{cases} \tag{11}$$

$$H^{\circ}_x = H^{\square}_x \quad \text{aperture.} \tag{12}$$

To enforce the boundary condition on the cavity sidewall—that is the vanishing of the tangential E-field—and the continuity of the electric field through the aperture, (11) is projected by using the cavity eigenfunctions $\phi^{\circ}_{p^e_m}(\varphi, x)$ over the cavity sidewall. On the contrary, the continuity equation of the magnetic field (12) is projected using the eigenfunctions $\phi^{\square}_q(x, y)$ on the aperture surface σ.

This leads, after substituting (2), (7), (3), and (8) in the two continuity equations, to the matrix equations

$$\begin{cases} \frac{1}{2}\mathbf{C} & = \mathbf{H}_{e_m}(\mathbf{A}^+ + \mathbf{A}^-) \\ \mathbf{H}^T_{e_m}\mathbf{Y}^{\circ}\mathbf{C} & = \mathbf{Y}^{\square}(\mathbf{A}^+ - \mathbf{A}^-) \end{cases} \tag{13}$$

where $\mathbf{A}^+ = [a^+_q]$, $\mathbf{A}^- = [a^-_q]$ and $\mathbf{C} = [c_p]$ are the incident, reflected and stationary modal amplitude vectors coefficients, $\mathbf{H}_{e_m}$ is the coupling matrix and $\mathbf{Y}^{\square}$ and $\mathbf{Y}^{\circ}$ are two diagonal square matrices of normalizing coefficient. Superscript 'T' denotes transpose. Note the 1/2 factor in the first of (13), resulting from the insertion of the electric and magnetic wall in the simmetry plane.

The elements of the coupling matrix are defined as

$$H_{e_m}(p, q) = \int_{\sigma} \phi^{\circ}_{p^e_m}(\varphi, x)\phi^{\square}_q(x, y)\, d\sigma \tag{14}$$

explicit form for which, always under the assumption of small b_i, is reported in Appendix, while

$$Y^{\square}_q = \int_{\sigma} h_{xq}\phi^{\square}_q(x, y)\, d\sigma = \frac{k^2 - k^2_{xm}}{\gamma_q}. \tag{15}$$

By solving the two matrix (13) as usual, the two scattering one port matrix $\mathbf{S}_e$ and $\mathbf{S}_m$ result

$$\mathbf{S}_{e_m} = \left(\mathbf{Y}^{\square} + 2\mathbf{H}^T_{e_m}\mathbf{Y}^{\circ}\mathbf{H}_{e_m}\right)^{-1}\left(\mathbf{Y}^{\square} - 2\mathbf{H}^T_{e_m}\mathbf{Y}^{\circ}\mathbf{H}_{e_m}\right) \tag{16}$$

and then the scattering matrix of the whole symmetric resonator is

$$\mathbf{S}_{11} = \frac{\mathbf{S}_m + \mathbf{S}_e}{2}$$

$$\mathbf{S}_{21} = \frac{\mathbf{S}_m - \mathbf{S}_e}{2}. \tag{17}$$

Note that $\mathbf{S}_{11}$ and $\mathbf{S}_{21}$ are real numbers because the irises operate below their cut-off frequency and the technique can be implemented using only real algebra.

B. Asymmetrical Cavity

The case of a cavity with rectangular apertures of different dimensions is now investigated. The most direct approach considers a symmetrical resonator with two apertures equal to the larger one followed by a symmetrical double-step to reduce the dimensions of one of the two apertures. The symmetrical resonator generalized scattering matrix must be therefore cascaded [12] to the double step one placed at a null distance from the aperture on the cavity sidewall.

This approach is quite simple because all the needed building-block are already available and one has only to combine them. However the computational cost is heavy, a great number of matrix operations are needed and the case of two apertures placed at different heights cannot be handled. The most powerful approach consists therefore in considering the whole resonator.

As for the symmetrical case, the continuity of the electric and magnetic fields in the two apertures must be enforced, toghether with the vanishing of the tangential electric field on the metallic sidewall of the cavity. The two equations are written as follows

$$j\omega\mu \sum_p c_p \phi^{\circ}_{p^e_m} = \begin{cases} \sum_q (a^+_{1q} + a^-_{1q})e_{1yq} + \sum_q (a^+_{2q} + a^-_{2q})e_{2yq} & \\ 0 & \text{(cavity sidewall)} \end{cases} \tag{18}$$

$$\sum_p c_p Y_p^{\circ} \phi_{p_m^e}^{\circ} = \sum_q (a_{1q}^+ - a_{1q}^-) h_{1xq} + \sum_q (a_{2q}^+ - a_{2q}^-) h_{2xq} \quad (19)$$

where the subscript 1 and 2 have been added to quantities relative to the first and second aperture, respectively.

Equation (18) must be projected on $\phi_{p_m^e}^{\circ}$ and the magnetic field-continuity (19) on $\phi_{1q}^{\square}$ and $\phi_{2q}^{\square}$ to solve the scattering problem. In matrix form, the three equations are

$$\begin{cases} \mathbf{H}_1(\mathbf{A}_1^+ + \mathbf{A}_1^-) + \mathbf{H}_2(\mathbf{A}_2^+ + \mathbf{A}_2^-) = \mathbf{C} \\ \mathbf{Y}_1^{\square}(\mathbf{A}_1^+ - \mathbf{A}_1^-) = \mathbf{H}_1^T \mathbf{Y}^{\circ} \mathbf{C} \\ \mathbf{Y}_2^{\square}(\mathbf{A}_2^- - \mathbf{A}_2^+) = \mathbf{H}_2^T \mathbf{Y}^{\circ} \mathbf{C} \end{cases} \quad (20)$$

and lead, after the elimination of the amplitude vector $\mathbf{C}$ to the generalized scattering matrix

$$\mathbf{S}_{11} = (\mathbf{Y}_1^{\square} + \mathbf{T})^{-1}(\mathbf{Y}_1^{\square} - \mathbf{T}) \quad (21)$$

$$\mathbf{S}_{12} = (\mathbf{Y}_1^{\square} + \mathbf{D})^{-1}\mathbf{F}^T(\mathbf{I} + \mathbf{S}_{22}) \quad (22)$$

$$\mathbf{S}_{21} = (\mathbf{Y}_2^{\square} + \mathbf{G})^{-1}\mathbf{F}(\mathbf{I} + \mathbf{S}_{11}) \quad (23)$$

$$\mathbf{S}_{22} = (\mathbf{Y}_2^{\square} + \mathbf{R})^{-1}(\mathbf{Y}_2^{\square} - \mathbf{R}) \quad (24)$$

where

$$\mathbf{T} = \mathbf{D} - \mathbf{F}^T(\mathbf{Y}_2^{\square} + \mathbf{G})^{-1}\mathbf{F} \quad (25)$$

and

$$\mathbf{R} = \mathbf{G} - \mathbf{F}(\mathbf{Y}_1^{\square} + \mathbf{D})^{-1}\mathbf{F}^T. \quad (26)$$

The two coupling matrices, whose coefficients are reported in Appendix, are

$$\mathbf{H}_1 = \begin{bmatrix} \mathbf{H}_{1e} \\ \mathbf{H}_{1m} \end{bmatrix} \quad \text{and} \quad \mathbf{H}_2 = \begin{bmatrix} \mathbf{H}_{2e} \\ \mathbf{H}_{2m} \end{bmatrix} \quad (27)$$

and

$$\begin{bmatrix} \mathbf{D} & \mathbf{F}^T \\ \mathbf{F} & \mathbf{G} \end{bmatrix} = \begin{bmatrix} \mathbf{H}_1^T \\ \mathbf{H}_2^T \end{bmatrix} \mathbf{Y}^{\circ} [\mathbf{H}_1 \quad \mathbf{H}_2]. \quad (28)$$

The simpler form for symmetrical cavity given in (16), (17) can be obtained by simply setting $\mathbf{Y}_1^{\square} = \mathbf{Y}_2^{\square}$ and $\mathbf{H}_1 = \mathbf{H}_2$ in the equations above. Also in this case only real algebra is needed.

III. Convergence Properties

In the mode-matching technique the field mode expansions are truncated for practical reasons and it is well known that the choice of the number of modes it is not always an easy matter. The extensive studies on the subject, both for a general discontinuity [20], [21] and for the iris-cavity discontinuity [10], demonstrated that the ratio between the number of modes used on each side of the junction plays a very important role in the convergence behavior of the mode matching technique. The best rate of convergence is obtained if the same spatial resolution of the field mode expansions in the two region forming the discontinuity is ensured [20]. This means that all the modes having a cut-off frequency lower than a prescribed value must be taken into account, both in the waveguide and in the cavity.

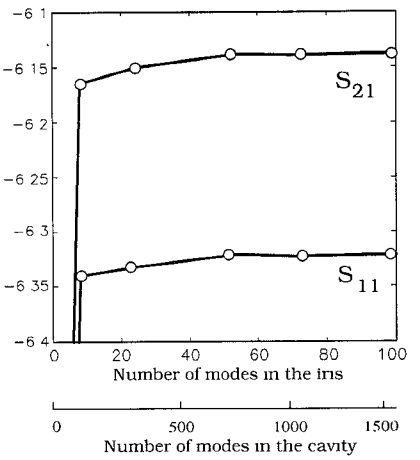

Fig. 3. Scattering coefficients convergence of a symmetrical cavity. See text for dimensions.

In the structure of Fig. 1 two convergence analysis have been carried out. The first one focuses the attention on the discontinuity between the rectangular iris and the cylindrical cavity (for the convergence behavior of the double-step discontinuity see [17], [21]). Fig. 3 shows the convergence of the reflection coefficient S_{11} and the transmission coefficient S_{21} (both are real numbers) as a function of the total number of modes in the iris and in the cavity. The dimensions of the considered cavity are $D = 34$ mm,$h = 18$ mm, $2\theta = 180°$, with two identical apertures of dimensions $a_i = 9$ mm and $b_i = 6$ mm. The analysis has been carried out at 13.8 GHz and shows that about 10 modes in the iris are sufficient to guarantee a value that differs less than 1% from the asymptotic one (obtained with 140 modes in the iris).

The second convergence analysis is devoted to the whole structure. A one-cavity filter is analyzed in order to study the influence of the various discontinuities. The accuracy in the evaluation of the resonant frequency and the quality factor of the loaded cavity, the two parameters on which the design of a filter is based, is discussed.

Fig. 4(a) and (b) show, respectively, the percent error on the quality factor Q and on the resonant frequency for the above mentioned cavity coupled to an external R120 (19.05×9.525 mm) rectangular waveguide. Three different coupling irises with lengths t_i are considered and the errors refers to the asymptotic values. It is interesting to note that the resonant frequency of the TE_{011}-mode is determined accurately even with very few modes in the iris while the evaluation of the Q-factor needs a more accurate analysis. Finally the convergence is faster for long irises (i.e., $t_i = 4$ mm) because of the weaker interaction of higher order modes between the double step discontinuity and the aperture in the cavity sidewall.

A further convergence analysis concerns the difference between the two approaches proposed for the analysis of an asymmetrical cavity. In Fig. 5 the same cavity as above but with two different irises with dimensions $a_1 = 9$ mm, $b_1 = 6$ mm, $a_2 = 8$ mm and $b_2 = 5$ mm is considered. The scattering coefficients are reported as a function of the number of modes used in the irises. The continuous lines represent the scattering coefficients obtained with (21) to (24), that is considering the

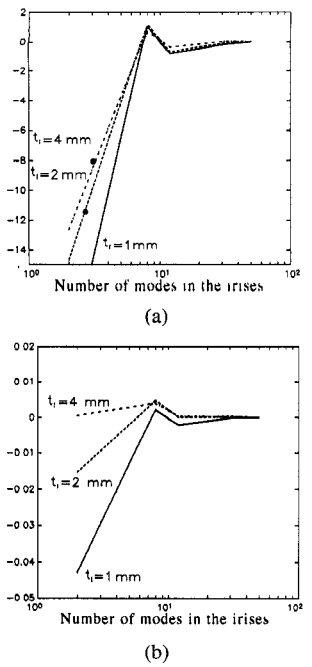

Fig. 4. (a) Quality factor Q: Percent error; convergence as a function of coupling iris length. (b) Resonant frequency: Percent error.

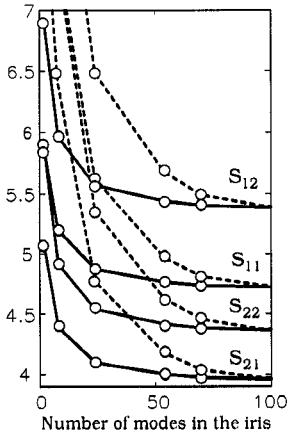

Fig. 5. Comparison between the rate of convergence of two approaches for the analysis of an asymmetrical cavity. Equations (21) to (24) in continuous line. Symmetrical cavity + double-step in broken line. See text for dimensions.

asymmetrical cavity as a whole, while the dashed lines show the results obtained by cascading a symmetrical cavity with a double-step to shrink one of the irises. The effectiveness of the former approach is supported by a much faster rate of convergence.

Concerning the computation speed, a comparison in terms of number of matrix multiplications and inversions is difficult to carry out because of the different matrix sizes. Equations (21) to (24) involve 4 matrix inversions and 11 matrix multiplications while only 2 inversions and 4 multiplications are needed to calculate the generalized scattering matrix of the symmetrical cavity. In addition to that, one must account for the cascading with the double-step discontinuity, which is a quite time-consuming process. In conclusion it was observed that the symmetrical cavity + double-step approach, although easy to implement, requires a large number of modes to obtain

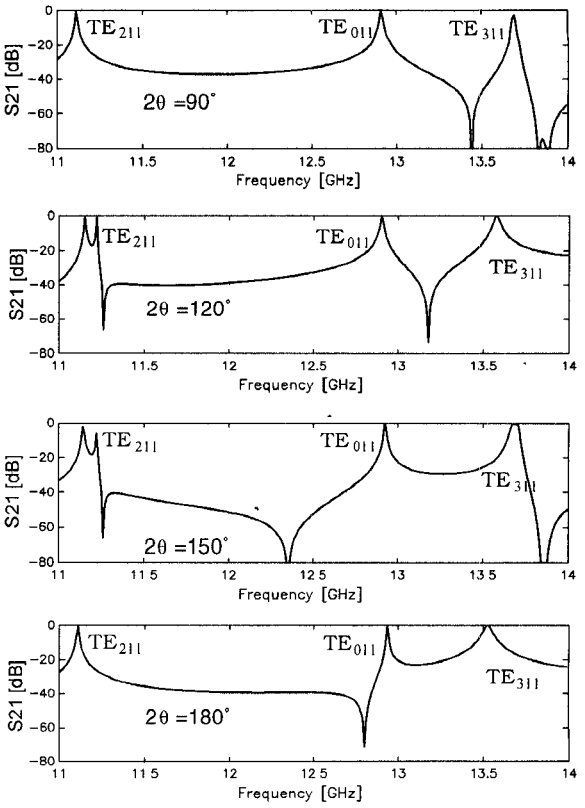

Fig. 6. Frequency response of a single cavity filter for different values of the angular offset 2θ. See text for structure dimensions.

a satisfactory accuracy of the solution and as a whole the direct method is less time-consuming.

IV. Numerical Results

A cavity with diameter $D = 34$ mm and height $h = 20.5$ mm, coupled by two identical irises with dimensions $a_i = 8$ mm, $b_i = 4$ mm and $t_i = 3$ mm to an external R120 waveguide is considered. The frequency response is reported in Fig. 6 for four values of the angle 2θ: $90°, 120°, 150°$ and $180°$. The TE_{211}, TE_{011} and TE_{311} resonant frequencies are cleary visible and transmission zeros too. The TE_{011} resonant frequency and the quality factor are only slightly affected by the irises position because of the angular uniformity of his fields while the TE_{211} and TE_{311} spurious modes frequency behavior depends in some way on this angle.

Also the frequency position of the transmission zeros strongly depends on the angle 2θ, as already observed by Kreinheder [22]. In his paper, Kreinheder explained accurately how and why nulls could appear between two resonant modes and shows, experimentally, that by controlling the angular offset of the apertures it is possible to place a transmission zero near the TE_{011} resonance and steepen the rejection slope. An interesting feature of these zeros is that their positions, relatively to the TE_{011} mode resonance, do not depend either on the irises dimensions or on the cavity ratio D/h, at least in the range $D/h = 1.38$ to 2.0, the most commonly used ratio range. The positions of the transmission zeros versus the angular offset are reported in Fig. 7. Both the null frequency between the TE_{211} and TE_{011} mode and between the TE_{011}

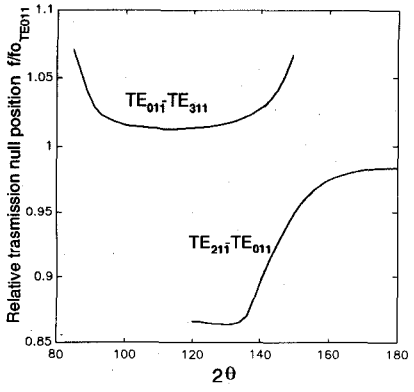

Fig. 7. Frequencies positions of the transmission zeros between TE_{211} and TE_{011} and between TE_{011} and TE_{311}-mode. The frequencies are normalized to the theoretical TE_{011} resonant frequency.

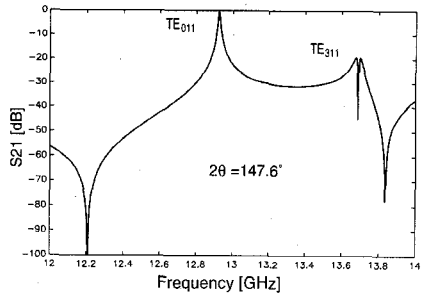

Fig. 8. TE_{311} spurious mode response partially suppressed by a transmission zero.

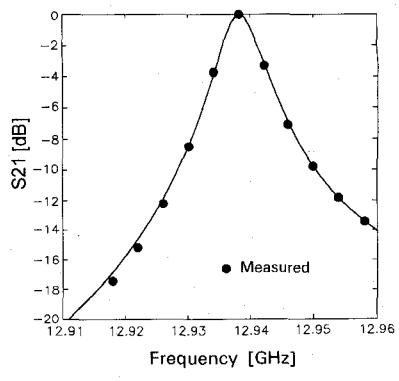

Fig. 9. Magnitude of S_{21} in dB versus frequency for the single cavity filter. Comparison between computed and measured response near the TE_{011} resonant frequency.

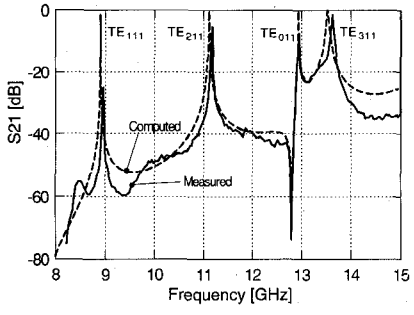

Fig. 10. Magnitude of S_{21} in dB versus frequency for the single cavity filter. Wide band comparison between computed and measured response.

and TE_{311} mode are reported. In the figure the null position is normalized to the theoretical TE_{011} resonant frequency. It must be noted that these nulls exist only for certain angles and vanish or move away outside these intervals. With an angle of about 147°, the two nulls are equally spaced from the TE_{011} and this permits an approximatively symmetrical insertion loss characteristic.

A further interesting numerical result is shown in Fig. 8. Even if there is not an angle that allows one to minimize at the same time the coupling with the TE_{211} and with the TE_{311} spurious mode, it's always possible to try to suppress the resonance of the TE_{311} by means of the transmission zero. For the above cited cavity for example, the angle $2\theta = 147.6°$ permits mantaining the TE_{311} response below 20 dB. This can be useful to increase the selectivity and the rejection in the design of bandpass filters.

V. Experimental Results

A number of prototype filters with one and four cavities have been realized and measured to test the proposed method of analysis.

The simpler prototype was a symmetrical single cavity filter with dimensions $a_i = 8$ mm, $b_i = 4$ mm, $D = 34$ mm, $h = 20.5$ mm. The cavity without apertures resonates at 13 GHz. The cavity was coupled to an R120 external rectangular waveguide by two 3 mm} long rectangular irises forming an angle $2\theta = 180°$. Only a simple tuning plunger has been included for tuning purposes, without any absorbing material beyond the movable endwall. The whole cavity was silver plated to reduce losses and the plunger was made non contacting with the cavity sidewalls in order to split the degeneracy between the TE_{011} and TM_{111} mode.

TABLE I
Four-Cavity Bandpass Filters' Dimensions [MM]

	D	a_i	b_i	t_1	t_2	t_3	h_1	h_2	$2\theta_1$	$2\theta_2$
This paper	15.0	4.6	2.0	2.852	7.757	8.630	9.911	9.956	90°	90°
[6]	15.0	4.6	2.0	3.310	6.102	6.846	10.882	10.882	-	-

A comparison between calculated and measured insertion-loss, obtained by a transmission and reflection test unit, is shown in Fig. 9 near the TE_{011} mode resonant frequency and in Fig. 10 over a very wide frequency band. Resonant frequencies of the TE_{111}, TE_{211}, TE_{011}, and TE_{311} modes are clearly visible, together with the transmission nulls due to mode interactions. Both figures shows an excellent agreement between calculated and measured response, not only near the TE_{011} resonant frequency band but all over the whole measured band. The discrepancies near the resonant frequencies of a spurious mode are essentially due to the movable tuning endwall.

This accurate method of analysis have been succesfully employed for the design of bandpass filters. An optimization program applying the evolution strategy method used in [13] varies the dimensions of the structure until the desired frequency response is obtained. The starting dimensions can be calculated resorting to the approximated techniques available in literature [6], [7], based on the small hole coupling theory [1], [3], [4] by Bethe.

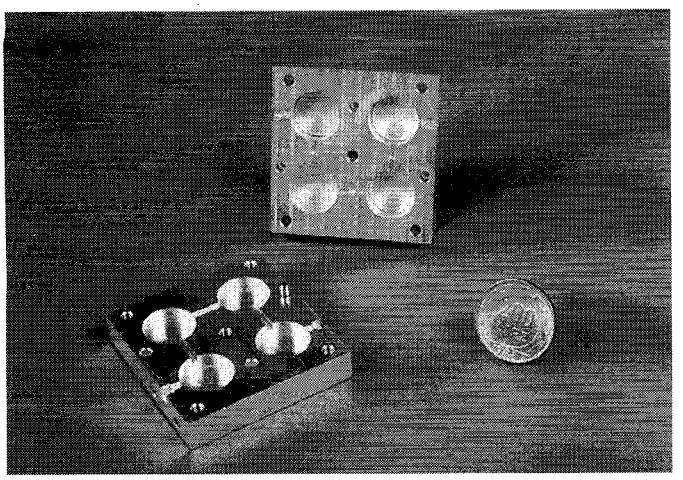

Fig. 11. Four cavity bandpass filter prototype.

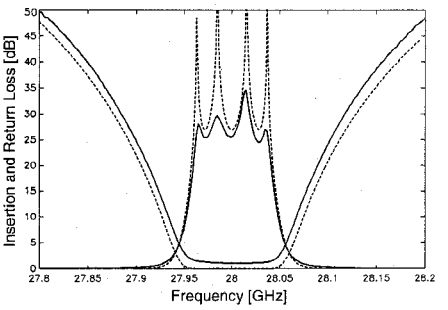

Fig. 12. Insertion and return loss in dB versus frequency for a four cavities filter (see Table I for dimensions). Comparison between computed (– – –) and measured (——) response.

A four cavity bandpass filter is shown in Fig. 11. The center frequency is 28 GHz and the bandwidth is 80 MHz. Table I reports filter dimensions before and after the optimization. Note that irises angles are not taken into account by the approximate design.

The prototype has been silver plated to reduce ohmic losses and include four tuning plungers and five small screws placed in the coupling irises. The comparison between measured and calculated insertion and return losses are reported in Fig. 12. The agreement is quite good and the ohmic losses at 28 GHz are limited to about 1 dB. The five screws were practically unused and it has been observed experimentally that the non touching plunger play a quite important role at these frequencies. A too large plunger is not efficient in splitting the resonant frequencies of TM_{111} and TE_{011} mode while a too small plunger also seriously affects the frequency behavior of the main mode. An experimentally accurate choice of this part is mandatory.

VI. Conclusion

The mode-matching technique have been used in this paper for the analysis of TE_{011} mode bandpass filter. The numerical method reported in this paper can overcome many limitations of the approximate models available in literature presently. Namely, it is now possible to examine the influence of the angle 2θ on the resonator frequency response, to determine accurately the position of other resonant spurious modes and transmission zeros and to take into account the higher order modes interactions between adjacent resonators. The only restriction on aperture dimensions is $b_i/R < 0.3$. Numerical properties of the technique have been widely discussed. Numerical and experimental results referring to a single cavity and a four cavity filters are presented too, showing a very good agreement between the measured and calculated frequency responses.

Appendix
Electrical and Magnetic Coupling Coefficients

Referring to Fig. 2 and (14) the coefficients of the electrical coupling matrix $\mathbf{H}_e$ are calculated. Expressions refer to a symmetrically placed aperture under the assumption of b_i small by respect R. Here a and b equal a_1, b_1—the dimensions of one aperture—when calculating $\mathbf{H}_1$ and a_2, b_2—the dimensions of the other aperture—when calculating $\mathbf{H}_2$. It is found

$$H_e(p,q) = \int_{\varphi_1}^{\varphi_2} R\, d\varphi \int_{-\frac{a}{2}}^{\frac{a}{2}} dx\, \phi_{pe}^{\circ}\, \phi_q^{\square} = \sqrt{\frac{2\epsilon_i\epsilon_n}{hRba\pi}}\, I_x I_{\varphi_e} \tag{29}$$

where $\varphi_1 = \theta \mp \sin^{-1}\frac{b}{2R} \simeq \theta \mp \frac{b}{2R}$. In the following, index $q = q(m,n)$ refers to the rectangular iris and $p = p(j,i)$ refers to the cavity.

$$I_x = \begin{cases} \frac{a}{2} & \text{if } k_{xm} = \kappa_{xj} \\ \frac{(-1)^m 2k_{xm}\cos(\kappa_{xj}\frac{a}{2})}{\kappa_{xj}^2 - k_{xm}^2} & \text{if } k_{xm} \neq \kappa_{xj} \end{cases} \tag{30}$$

where $k_{xm} = (2m+1)\pi/a$ and $\kappa_{xj} = (2j+1)\pi/h$ and

$$I_{\varphi_e} = \begin{cases} \frac{b}{\epsilon_n}\cos(\frac{n\pi}{2} - k_{yn}R\theta) & \text{if } i = k_{yn}R \\ \frac{iR[(-1)^n \sin(i\theta+\frac{ib}{2R}) - \sin(i\theta-\frac{ib}{2R})]}{i^2-(k_{yn}R)^2} & \text{if } i \neq k_{yn}R \end{cases} \tag{31}$$

where $k_{yn} = \frac{n\pi}{b}$.

The coefficients of the magnetic coupling matrix $\mathbf{H}_m$ are calculated in the same way

$$H_m(p,q) = \int_{\varphi_1}^{\varphi_2} R\, d\varphi \int_{-\frac{a}{2}}^{\frac{a}{2}} dx\, \phi_{pm}^{\circ}\, \phi_q^{\square} = \sqrt{\frac{2\epsilon_i\epsilon_n}{hRba\pi}}\, I_x I_{\varphi_m} \tag{32}$$

where I_x is given by (30) and

$$I_{\varphi_m} = \begin{cases} \frac{b}{2}\sin(-\frac{n\pi}{2} + \frac{n\pi R\theta}{b}) & \text{if } i = k_{yn}R \\ \frac{iR[\cos(i\theta-\frac{ib}{2R}) - (-1)^n\cos(i\theta+\frac{ib}{2R})]}{i^2-(k_{yn}R)^2} & \text{if } i \neq k_{yn}R. \end{cases} \tag{33}$$

Acknowledgment

The authors wish to thank Siemens Telecomunicazioni S.p.a, Milano, Italy, and in particular Ing. A. Giavarini, who supported the realization and measurements of prototypes.

References

[1] H. A. Bethe, "Theory of diffraction by small holes," *Phys. Rev.*, vol. 66, pp. 163-182, Oct. 1944.
[2] S. B. Cohn, "Microwave coupling by large apertures," *Proc. IRE*, vol. 40, pp. 696–699, June 1952.
[3] N. A. McDonald, "Electric and magnetic coupling through small apertures in shield walls of any thickness," *IEEE Trans. Microwave Theory Tech.*, vol. MTT-20, pp. 689–695, Oct. 1972.

[4] N. A. McDonald, "Simple approximations for the longitudinal magnetic polarizabilities of some small apertures," *IEEE Trans. Microwave Theory Tech.*, vol. 36, p. 1141, July 1988.
[5] R. Levy, "Improved single and multiaperture waveguide coupling theory, including explanation of mutual interactions," *IEEE Trans. Microwave Theory Tech.*, vol. MTT-28, p. 331, Apr. 1980.
[6] G. L. Matthaei, L. Young, and E. M. T. Jones, *Microwave filters impedance-matching networks and coupling structures.* New York: McGraw-Hill, 1964.
[7] F. Shnurer, "Design of aperture-coupled filters," *IRE Trans. Microwave Theory Tech.*, pp. 238–243, Oct. 1957.
[8] A. E. Atia and A. E. Williams, "General TE_{011}-mode waveguide bandpass filters," *IEEE Trans. Microwave Theory Tech.*, vol. MTT-24, pp. 640–648, Oct. 1964.
[9] H. L. Thal, "Cylindrical TE_{011}/TM_{111} mode control by cavity shaping," *IEEE Trans. Microwave Theory Tech.*, vol. MTT-27, pp. 982–986, Dec. 1979.
[10] A. Melloni, "Filtri a Cavitá Surmodate Direttamente Accoppiate: Analisi e Sintesi," Ph.D. Dissertation, Politecnico di Milano, Italy, Nov. 1992.
[11] A. Melloni, M. Politi, G. G. Gentili, and G. Macchiarella, "Field design of TE_{011}-mode waveguide bandpass filters," in *Proc. 22nd European Microwave Conf.*, Helsinki, Aug. 1992, pp. 533–538.
[12] T. Itoh, *Numerical Techniques for Microwave and Millimeter-Wave Passive Structures.* New York: Wiley, 1989.
[13] H. Patzelt and F. Arndt, "Double-plane steps in rectangular waveguides and their application for transformers, irises and filters," *IEEE Trans. Microwave Theory Tech.*, vol. MTT-30, pp. 771–776, May 1982.
[14] R. Safavi-Naini and R. H. MacPhie, "Scattering at rectangular to rectangular waveguide junctions," *IEEE Trans. Microwave Theory Tech.*, vol. MTT-30, pp. 2060–2063, Nov. 1982.
[15] Y. C. Shih and K. C. Gray, "Convergence of numerical solutions of step-type waveguide discontinuity problems by modal analysis," in *1983 IEEE MTT-S Int. Microwave Symp. Dig.*, pp. 233–234.
[16] J. Bornemann and R. Vahldieck, "Characterizations of a class of waveguide discontinuities using a modified TE^x_{mn} mode approach," *IEEE Trans. Microwave Theory Tech.*, vol. 38, pp. 1816–1821, Dec. 1990.
[17] G. G. Gentili, A. Melloni, G. Macchiarella, and M. Politi, "Analysis of double-step discontinuity in rectangular waveguide using a TE^x-TM^x field expansion," *Microwave Opt. Technol. Lett.*, vol. 6, pp. 358–361, May 1993.
[18] C. G. Montgomery, R. H. Dicke and E. M. Purcell, "Principles of microwave circuits," in *Radiation Laboratory Series.* New York: McGraw-Hill, 1948.
[19] M. Abramowitz and I. A. Stegun, *Handbook of Mathematical Functions.* New York: Dover.
[20] R. Sorrentino, M. Mongiardo, F. Alessandri, and G. Schiavon, "An investigation of the numerical properties of the mode-matching technique," *Int. J. Numerical Modelling*, vol. 4, pp. 19–43, Apr. 1991.
[21] G. G. Gentili and A. Melloni, "Un Algoritmo per la scelta ottima dei modi nelle tecniche di mode-matching," *Acta X Riunione Nazionale di Elettromagnetismo*, pp. 389–392, 1994.
[22] D. E. Kreinheder and T. D. Lingren: "Improved selectivity in cylindrical TE_{011} filters by TE_{211}/TE_{311} mode control," *IEEE Trans. Microwave Theory Tech.*, vol. MTT-30, pp. 1383–1387, Sept. 1982.

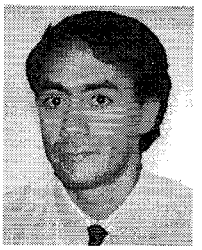

Andrea Melloni was born in Milano, Italy, in 1963. He graduated in electronic engineering, and received the Ph.D. degree in electronic engineering in 1992 from the Politecnico di Milano, Italy.

In 1989 he joined the Department of Electronic at the same university. Since then he has been an Assistant Professor in the Department of Electronics. His current research activities concern with numerical methods for analysis, modeling, and design of passive microwave and millimeter-wave structures.

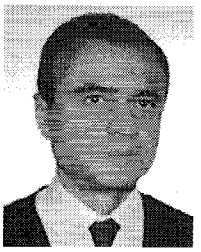

Marco Politi was born near Milan, Italy, in 1951. He received the Dr. Ing. degree in electronic engineering from the Politecnico di Milano, Milan, Italy, in 1976.

From 1977 to 1983 he was with the Centro di Studio per le Telecomunicazioni Spaziali of the National Research Council of Italy CNR at the Politecnico di Milano, working in the field of centimeter-wave propagation. In 1983 he joined the Politecnico di Milano as an Assistant Professor. Since 1991 he has been Associate Professor of Electromagnetic Fields at the Dipartimento di Elettronica e Informazione of the same university. His research activity is now mainly concerned with the analysis and design of microwave and millimeter-wave devices for telecommunication applications, and with the numerical methods for the solution of related electromagnetic problems.

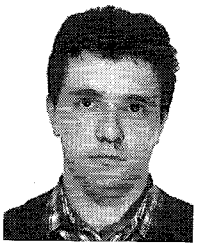

Gian Guido Gentili was born in Turin, Italy, in 1961. He received the "laurea" degree in electronic engineering from Politecnico di Milano, Milano, Italy, in 1987.

From 1987 to 1989 he worked at Politecnico di Milano as a scholarship holder, developing CAD tools for the electromagnetic analysis of microstrip circuits. In 1989, as a researcher, he joined the "Centro di Studio sulle Telecomunicazioni Spaziali" CSTS-CNR, which resides at Politecnico di Milano. Since then he has been working on the application of numerical methods for the modelling and design of microwave and millimeter wave passive structures.